AIP | Applied Physics Letters

Low-temperature synthesis of ZnSe nanowires and nanosaws by catalyst-assisted molecular-beam epitaxy

A. Colli, S. Hofmann, A. C. Ferrari, C. Ducati, F. Martelli et al.

Citation: Appl. Phys. Lett. **86**, 153103 (2005); doi: 10.1063/1.1897053
View online: http://dx.doi.org/10.1063/1.1897053
View Table of Contents: http://apl.aip.org/resource/1/APPLAB/v86/i15
Published by the American Institute of Physics.

Low-temperature synthesis of ZnSe nanowires and nanosaws by catalyst-assisted molecular-beam epitaxy

A. Colli,[a] S. Hofmann, and A. C. Ferrari
Department of Engineering, University of Cambridge, Cambridge CB2 1PZ, United Kingdom

C. Ducati
Department of Materials Science and Metallurgy, University of Cambridge, Cambridge, United Kingdom

F. Martelli,[b] S. Rubini, S. Cabrini, and A. Franciosi[c]
Laboratorio Nazionale TASC-INFM, Area Science Park, 34012 Trieste, Italy and Centre of Excellence for Nanostructured Materials, University of Trieste, 34127 Trieste, Italy

J. Robertson
Department of Engineering, University of Cambridge, Cambridge CB2 1PZ, United Kingdom

(Received 8 November 2004; accepted 15 February 2005; published online 4 April 2005)

Single-crystal ZnSe nanowires are grown on a prepatterned gold catalyst by molecular-beam epitaxy. Optimum selectivity and maximum nanowire densities are obtained for growth temperatures in the range 400–450 °C, but gold-assisted growth is demonstrated for temperatures as low as 300 °C. This suggests a diffusion process on/through the catalyst particle in the solid state, in contrast to the commonly assumed liquid phase growth models. Straight wires, as thin as 10 nm, nucleate together with thicker and saw-like structures. A gold particle is always found at the tip in both cases. © *2005 American Institute of Physics*. [DOI: 10.1063/1.1897053]

One-dimensional (1D) semiconductor nanostructures are receiving increasing attention because of their potential applications in electronics and photonics.[1,2] Device performance typically depends on the material structure and crystallinity, but nano-object assembly is also a critical issue for applications. Direct manipulation of nanostructures into devices is difficult and expensive. Thus, the full potential of nanostructures will only be realized when they can be directly grown into devices. This requires a deep understanding and accurate control of the growth processes. Low growth temperatures would widen the range of possible substrates, including more delicate materials such as polymers.[3,4]

Fabrication of several types of 1D nanostructures, such as nanowires (NWs), nanorods, and nanoribbons, has been demonstrated for elemental semiconductors, such as Si and Ge, as well as for III-V and II-VI compounds. Among II-VI semiconductors, ZnSe and related alloys are known to be suitable materials for blue-green light emission. ZnSe NWs deposition has been reported using vapor phase growth,[5] metalorganic chemical vapor deposition,[6,7] molecular-beam epitaxy (MBE),[8] and thermochemical processes.[9]

MBE is currently the technique of choice to fabricate ZnSe-based lasers with best performance and lifetimes.[10] However, it has rarely been used for NW synthesis. Compared to many other deposition techniques, MBE allows an extremely accurate control of the growth parameters and therefore is the ideal method to study the growth of nanomaterials. Chan *et al.*[8] reported MBE growth of ZnSe NWs on GaP(111) substrates with a Au catalyst using a ZnSe compound-source effusion cell. They proposed the minimum growth temperature for ZnSe NWs to be 530 °C, which was argued to allow the formation of a liquid Au-Zn-Se eutectic, as required by the vapor-liquid-solid (VLS) nucleation model.[5,8,11] Such a temperature was argued to allow the formation of a liquid Au-Zn-Se eutectic[8] from which the NW would nucleate—at the liquid-solid interface—upon supersaturation of the alloy with the impinging gaseous reactants.[5,8,11] However, it is known that optimum MBE growth temperatures for epitaxial ZnSe layers are close to 300 °C, since higher temperatures degrade the optical properties of the material.[12] Thus, the MBE growth temperature of ZnSe NWs needs to be significantly lowered as compared to Ref. 8.

Here we show that the controlled formation of 1D ZnSe nanostructures by catalyst-assisted MBE is possible at much lower growth temperatures than previously proposed. Optimum selectivity and maximum NW densities are obtained for growth temperatures in the range 400–450 °C. However, NWs with relatively high aspect ratios are observed for growth temperatures as low as 300 °C. As a consequence, we suggest a growth mechanism governed by diffusion processes on or through a solid Au catalyst, in contrast to the generally assumed VLS model.

All samples were grown by solid-source MBE using equipment and methods that have been utilized for the synthesis of a variety of state-of-the-art II-VI heterostructures. For NWs growth, elemental Zn and Se were evaporated on the sample surface for 1 h, with a II/VI beam pressure ratio of 0.4, corresponding to an equivalent two-dimensional ZnSe growth rate of 0.45 μm/h.

Figure 1 shows field-emission scanning electron microscopy (FE-SEM) plan-view images of ZnSe 1D nanostructures grown on *n*-doped Si(100) wafers coated with a 20-nm-thick SiO_2 sputtered layer. A thin 0.5–1.5 nm Au film was thermally evaporated onto the SiO_2 surface[13] and patterned using ultraviolet and e-beam lithography prior to loading the substrates in the MBE chamber. Figures 1(a)–1(d) show samples grown at substrate temperatures T_g=300, 400, 450, and 550 °C. The boundary region between the Au pattern and the bare SiO_2 substrate is shown in all cases.

[a]Electronic mail: ac458@cam.ac.uk
[b]Electronic mail: martelli@tasc.infm.it
[c]Also at: Dipartimento di Fisica, Universita' di Trieste, 34127 Trieste, Italy.

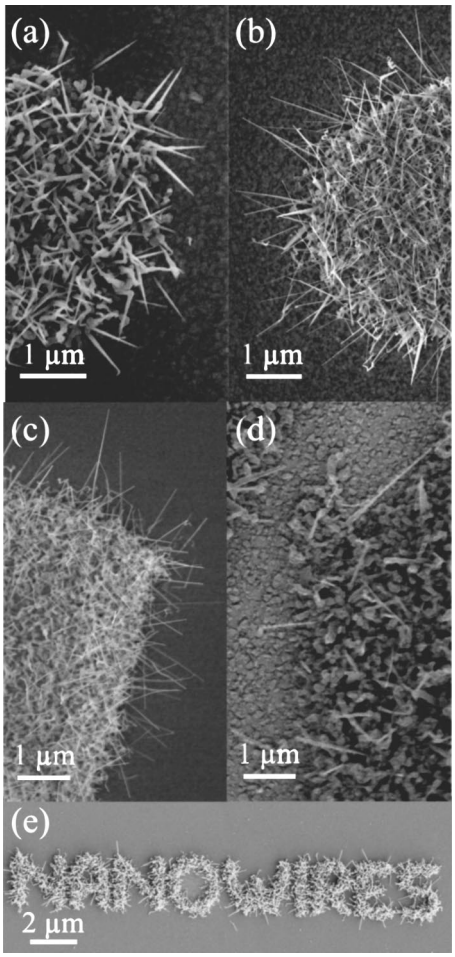

FIG. 1. Plan-view FE-SEM images of ZnSe nanostructures showing the boundary region between the Au-pattern and the barc SiO_2/Si substrate. Growth temperatures are (a) 300 °C; (b) 400 °C; (c) 450 °C; (d) 550 °C. (e) Demonstration of process selectivity at 450 °C.

At 300 °C [see Fig. 1(a)], thin, constant-diameter NWs with high aspect ratio, as well as tapered, triangularly shaped nanostructures, are observed. For growth temperatures in the 400–450 °C range [see Figs. 1(b) and 1(c)], larger densities of longer, straight, and thinner NWs nucleate from the Au pattern and extend to the surrounding areas. Very few tapered nanostructures are observed. At 550 °C [see Fig. 1(d)], the NW density is significantly lower. *In situ* x-ray photoelectron spectroscopy (XPS), as well as energy dispersion x-ray spectra (not shown), confirm the formation of stoichiometric ZnSe for the whole range of growth temperatures explored.

Figure 1(e) graphically illustrates the high degree of selectivity of the Au-catalyzed process and the optimum NW morphology and density at 450 °C. ZnSe NWs only grow on the lithographically predefined Au "nanowire" pattern. In order to further quantify the selectivity of the growth, we probed the *total* coverage of ZnSe on the catalyst-free regions by means of XPS and photoluminescence (PL). Only relatively thin layers of ZnSe (at most a few nanometers thick) were observed by XPS for growth temperatures down to 400 °C, while no PL emission was seen for Au-free areas. At T_s=300 °C, higher amounts of ZnSe were found on Au-free surface regions, and a small PL signal was also detected. We stress that, despite the presence of Zn and Se XPS signal, no tridimensional structures were observed on catalyst-free regions, in the whole range of growth conditions investigated.

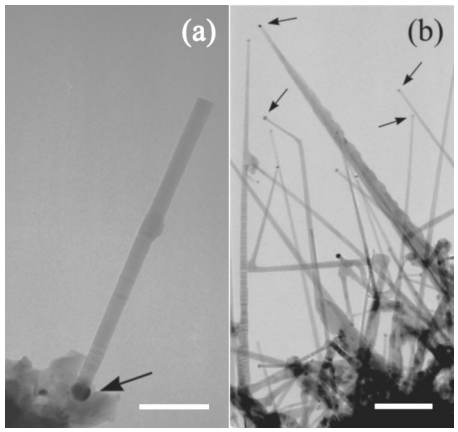

FIG. 2. (a) Bright-field TEM image of a single ZnSe NW scratched off the Si substrate. Scalebar 50 nm. (b) Bright-field TEM image of as-grown NWs and nanosaws on the edge of a Mo TEM grid. Metallic droplets of similar size (~10–20 nm) are always visible at the tip. Scalebar 200 nm.

The crystalline morphology of the 1D ZnSe nanostructures, was probed by a JEOL 4000Fx transmission electron microscope (TEM) operated at 400 kV. To prepare the TEM samples we used two different strategies. One is to scratch the as-grown ZnSe NWs off the Si(001) substrate to transfer them onto the TEM grid. Alternatively, we grew NWs at 450 °C directly on a Mo TEM grid, to allow a detailed and accurate analysis of the as-deposited NWs. A 20-nm-thick SiO_2 layer was sputtered on both sides of the grid. A thin Au film (0.5–1.5 nm thick) was then thermally evaporated onto the surface facing the MBE fluxes. By scratching the NWs off the Si substrate, we generally obtain only a low density of measurable nanostructures. In addition, some of these are often only partial sections of broken wires, missing important information on their overall morphology. Figure 2(a) shows, for example, a bright-field TEM image of a single NW scratched off the Si substrate. We emphasize that it is often not straightforward to detect the catalyst particle, nor to conclude if a tip-growth or base-growth mechanism has taken place. We get much clearer results by examining the NWs directly grown on a TEM grid edge [Fig. 2(b)]. Here, the number of observable NWs is far higher, and two competing 1D morphologies are clearly seen. Most of the nanostructures are micrometer-long wires, with diameters as low as 10 nm. Some larger and tapered nanosaws, with one (or more) irregular edge(s), are also found. As indicated by the arrows in Fig. 2(b), Au nanoparticles are *always* detected at the tip of *both types* of nanostructures.

Figure 3 shows high-resolution TEM micrographs of the two types of ZnSe nanostructures grown at 450 °C. The lattice imaging in Fig. 3(a) reveals the single-crystal nature of a straight NW, 9 nm thick. The parallel fringes are tentatively assigned to the zinc-blende {111} planes (3.276 Å), in agreement with previous reports on ZnSe NWs grown along the (111) direction.[5] The same high crystallinity is found for nanostructures grown at 300 °C, but their average diameter is typically higher. Figure 3(b) shows a highly crystalline tapered nanosaw about 40 nm wide at the base and 10 nm wide at the tip. Large-angle grain boundaries due to different crystallographic twinning appear related with the formation of the saw teeth [see inset, Fig. 3(b)], which are typically 8 to 10.5 nm deep. The lattice fringes correspond to the {111} planes of zinc-blende ZnSe. Within the experimental uncertainty, however, the plane spacing in Figs. 3(a) and 3(b)

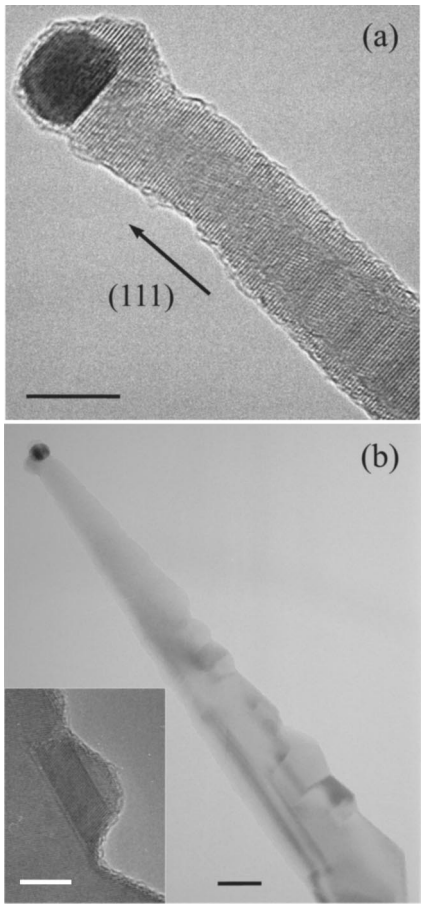

FIG. 3. High-resolution TEM images of ZnSe nanostructures grown at 450 °C. (a) Representative single-crystal straight NW ~9 nm in diameter; (b) A triangularly shaped nanosaw with a single irregular edge. (Inset) A close-up of a tooth of a crystalline nanosaw. Scalebars are (a)10 nm, (b) 20 nm, (Inset) 10 nm.

could also be consistent with a wurzite ZnSe structure. Electron energy loss spectroscopy shows that all the structures are always surrounded by a thin oxide layer, probably formed following exposure to atmosphere.

The VLS mechanism is often used to describe catalytic growth of semiconductor NWs. Liquid metallic droplets of a catalyst present on the substrate would alloy with the impinging gaseous reactants.[11] The minimum growth temperature in the VLS model is given by the (size-corrected) eutectic point of the wire and catalyst elements. For Au-catalyzed ZnSe NW growth on GaP(111), Chan *et al.*[8] proposed 530 °C as the minimum possible growth temperature.

Here, we demonstrate a ZnSe NW growth temperature as low as 300 °C. Such a temperature is far lower than the Au-ZnSe eutectic temperature quoted in Ref. 8 (530 °C), and well below the eutectic temperatures found in the Au-Zn binary phase diagrams (650–683 °C).[14] Furthermore, the size of our Au particles (10–20 nm) is still too big to produce a massive drop in the melting temperature.[15] The Au-Se binary phase diagram does not exhibit an eutectic point, but only stoichiometric compounds with comparatively high melting temperatures.[14] We therefore suggest that the Au catalyst particle is in the solid state during our low-temperature growth of ZnSe NWs, and that a solid-phase diffusion process, either in the bulk or on the surface, or both, must be responsible for NW nucleation. Our findings are conceptually similar to a previous report by Kamins *et al.*[16] of Ti-promoted Si NW growth for temperatures below the Si-Ti eutectic point, and to what was previously found for the low-temperature catalytic growth of carbon nanofibers.[3,17] A solid-state diffusion mechanism was also recently proposed[18] to explain the Au-catalyzed growth of GaAs NWs by chemical-beam epitaxy. MBE occurs in conditions far from thermodynamic equilibrium; thus, *in situ* investigations of the NW growth steps will be necessary to conclusively address the details of the growth mechanism.

We further suggest that the growth of the ZnSe nanosaws happens via the nucleation of a straight Au-catalyzed NW with the size of the Au droplet determining its initial diameter, followed by an additional epitaxial growth of ZnSe on the wire sides. A similar idea was proposed for CdSe nanosaws grown by thermal evaporation,[19] and would explain the triangular profile of the thickest nanostructures. The controlled formation of nanosaws could have very important device applications, since the varying surface potential in nanosaws could define "natural" nanodots isolated by tunnel barriers due to surface depletion. So far, such multiple quantum dot structures have been fabricated only by using complicated nanolithography processes.[20]

In summary, we reported the MBE Au-catalyzed, selected-area growth of ZnSe NWs several micrometers long and 9–10 nm wide. High-quality ZnSe NWs are obtained at temperatures as low as 300 °C, a potentially important step in the improvement of their optical quality and integration.

This work was supported by the EU project CARDECOM. We thank Z. A. K. Durrani for useful discussion. A. C. F. acknowledges funding from The Royal Society.

[1]Y. Cui, Q. Wei, H. Park, and C. M. Lieber, Science **293**, 1289 (2001).
[2]M. Law, J. Goldberger, and P. Yang, Annu. Rev. Mater. Sci. **34**, 83 (2004).
[3]S. Hofmann, C. Ducati, J. Robertson, and B. Kleinsorge, Appl. Phys. Lett. **83**, 135 (2003); **83**, 4661 (2003).
[4]W. U. Huynh, J. J. Dittmer, and A. P. Alivisatos, Science **295**, 2425 (2002).
[5]B. Xiang, H. Z. Zhang, G. H. Li, F. H. Yang, F. H. Su, R. M. Wang, J. Xu, G. W. Lu, X. C. Sun, Q. Zhao, and D. P. Yu, Appl. Phys. Lett. **82**, 3330 (2003).
[6]X. T. Zhang, Z. Liu, Y. P. Leung, Quan Li, and S. K. Hark, Appl. Phys. Lett. **83**, 5533 (2003).
[7]X. T. Zhang, K. M. Ip, Z. Liu, Y. P. Leung, Quan Li, and S. K. Hark, Appl. Phys. Lett. **84**, 2641 (2004).
[8]Y. F. Chan, X. F. Duan, S. K. Chan, I. K. Sou, X. X. Zhang, and N. Wang, Appl. Phys. Lett. **83**, 2665 (2003).
[9]Y.-C. Zhu and Y. Bando, Chem. Phys. Lett. **377**, 367 (2003).
[10]E. Kato, H. Noguchi, M. Nagai, H. Okuyama, S. Kijima, and A. Ishibashi, Electron. Lett. **34**, 282 (1998).
[11]R. S. Wagner and W. C. Ellis, Appl. Phys. Lett. **4**, 89 (1964).
[12]J. M. DePuydt, H. Cheng, J. E. Potts, T. L. Smith, and S. K. Mohapatra, J. Appl. Phys. **62**, 4756 (1987).
[13]S. Hofmann, C. Ducati, R. J. Neill, S. Piscanec, A. C. Ferrari, J. Geng, R. E. Dunin-Borkowski, and J. Robertson, J. Appl. Phys. **94**, 6005 (2003).
[14]T. B. Massalski, *Binary Alloy Phase Diagrams*, 2nd ed., (ASM International, Materials Park, Ohio, 1990), Vol. 1.
[15]P. Buffat and J. P. Morel, Phys. Rev. A **13**, 2287 (1976).
[16]T. I. Kamins, R. S. Williams, D. P. Basile, T. Hesjedal, and J. S. Harris, J. Appl. Phys. **89**, 1008 (2001).
[17]S. Helveg, C. Lopez-Cartes, J. Sehested, P. L. Hansen, B. S. Clausen, J. R. Rostrup-Nielsen, F. Abild-Pedersen, and J. K. Norskov, Nature (London) **427**, 426 (2004).
[18]A. I. Persson, M. W. Larsson, S. Stenström, B. J. Ohlsson, L. Samuelson, and L. R. Wallenberg, Nat. Mater. **3**, 677 (2004).
[19]C. Ma, Y. Ding, D. Moore, X. Wang, and Z. L. Wang, J. Am. Chem. Soc. **126**, 708 (2004).
[20]P. A. Cain, H. Ahmed, and D. A. Williams, J. Appl. Phys. **92**, 346 (2002).